Available online at www.sciencedirect.com
SCIENCE DIRECT®
Vacuum 73 (2004) 327–332
VACUUM
SURFACE ENGINEERING, SURFACE INSTRUMENTATION & VACUUM TECHNOLOGY
www.elsevier.com/locate/vacuum

Micro-structured electrode arrays: high-frequency discharges at atmospheric pressure—characterization and new applications

Lutz Baars-Hibbe[a], Christian Schrader[a], Philipp Sichler[b], Thorben Cordes[a], Karl-Heinz Gericke[a,*], Stephanus Büttgenbach[b], Siegfried Draeger[c]

[a] *Institut für Physikalische and Theoretische Chemie, Technische Universität Braunschweig, Hans-Sommer-Straße 10, D-38106 Braunschweig, Germany*
[b] *Institut für Mikrotechnik, Technische Universität Braunschweig, Alte Salzdahlumer Str. 203, D-38124 Braunschweig, Germany*
[c] *Institut für Mikrobiologie, Technische Universität Braunschweig, Spielmannstraße 7, D-38106 Braunschweig, Germany*

Abstract

Micro-structured electrode (MSE) arrays allow to generate large-area uniform glow discharges over a wide pressure range up to atmospheric pressure. The electrode dimensions in the μm-range realized by means of modern micro-machining and galvanic techniques are small enough to generate sufficiently high electric field strengths to ignite gas discharges applying only moderate radio frequency (RF, 13.56 MHz) voltages (80–390 V in Ne, He, Ar and N_2). The non-thermal plasma system is characterized by a special probe measuring the electric parameters. The MSE-driven plasmas show a different behavior from conventional discharge plasmas depending on the pressure and the type of gas. With the MSE arrays as plasma sources, several applications were developed and successfully tested: Plasma chemistry (decomposition of waste gases like CF_4) and thin film deposition (e.g. SiO_2 layers on various substrates). A new atmospheric pressure application realized in our lab is the sterilization of food packaging materials.

Keywords: Micro-structured electrodes; Atmospheric pressure plasma; Radio frequency discharges; Paschen law; Sterilization

1. Introduction

Non-thermal plasma processing techniques optimized for atmospheric pressure applications are the subject of a recent growing interest due to their significant industrial advantages. At atmospheric pressure, thin film depositions with very high rates are possible and cost-intensive vacuum technology is avoided. There are many approaches published recently (see [1,2] and references therein) to overcome the problems to generate and sustain a stable uniform non-thermal atmospheric plasma.

Recently, micro-structured electrode (MSE) arrays were introduced as alternative atmospheric pressure plasma sources [3,4]. They consist of a system of planar and parallel electrodes (comb structure, see Fig. 1) arranged on an insulating substrate and manufactured by means of modern micro-machining and galvanic techniques. The electrode dimensions, especially the electrode gap width, in the μm-range are small enough to

*Corresponding author. Fax: +49-531-391-5396.
E-mail address: k.gericke@tu-bs.de (K.-H. Gericke).

0042-207X/$ - see front matter © 2004 Elsevier Ltd. All rights reserved.
doi:10.1016/j.vacuum.2003.12.107

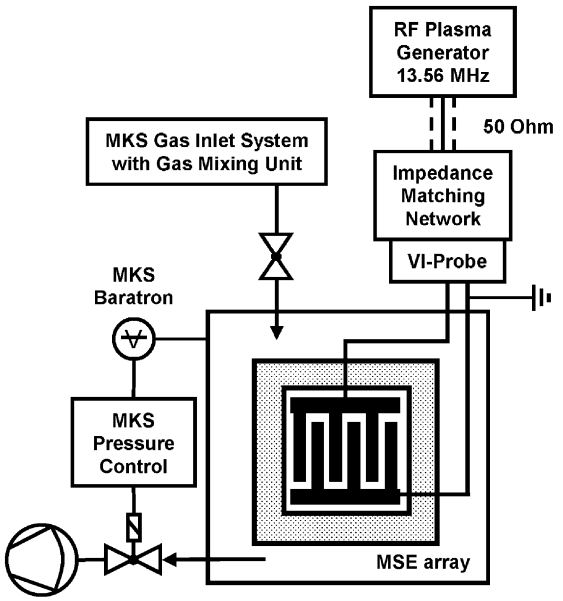

Fig. 1. Scheme of the experimental setup. Gas inlet system and vacuum system published in detail in Ref. [4].

generate sufficiently high electric field strengths to ignite gas discharges applying only moderate radio frequency (RF, 13.56 MHz) voltages (less than 400 V).

In this publication, we characterize the ignition parameters of the MSE-driven RF plasmas and demonstrate their special behavior, which differs from conventional discharges. With the gained knowledge, we are able to design new optimized MSE arrays. Additionally, we present new applications realized in our lab; for example, the sterilization of food packaging materials.

2. Experimental setup

The MSE arrays are studied as a non-thermal high-frequency plasma source with the experimental setup schematically shown in Fig. 1. The gas inlet system and vacuum system are described in detail elsewhere [1,2,4]. A gas flow rate between 50 and 300 sccm was set up by means of mass flow controllers. In all experiments of Section 3, a constant gas flow of 200 sccm Ne, He, Ar or N_2 was used. The discharges were generated using an

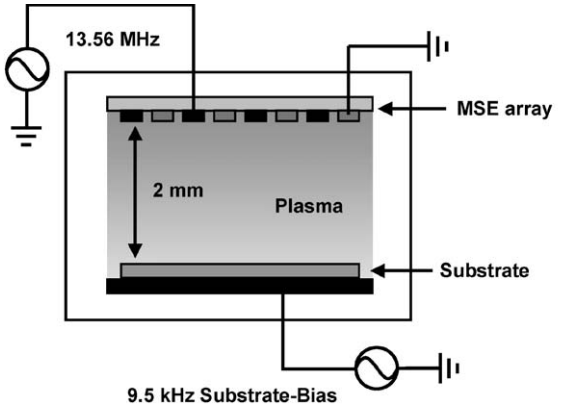

Fig. 2. Scheme of the sterilization and deposition setup.

RF power supply at 13.56 MHz (ENI ACG-3B) equipped with a matching network (ENI MW-5D). Between the matching network and the MSE array, a special probe (ENI VI-Probe) is inserted in order to measure voltage, current and phase angle of the system.

The sterilization and deposition setup shown in Fig. 2 consists of the experimental setup to ignite RF gas discharges described above (Fig. 1) and an additional electrode plate coplanary installed to the MSE array at a distance of 2 mm. A substrate (Si, Cu or different plastic films) is mounted on this electrode, which is biased with a 9.5 kHz AC potential of 500–1300 Vpp. The applied sine potential is monitored with an oscilloscope. With a diode, the AC bias can be rectified to a pulsed negative DC-(−) bias or a pulsed positive DC-(+) bias.

3. Characterization of the MSE plasma

The dimensions of the MSE arrays are an electrode gap width d of 70 μm, an electrode thickness of 100 μm and a width of 1350 μm (electrode material: Cu/Ni). The electrode gap has a complex geometry with incorporated protrusions [5] allowing to generate large-area uniform glow discharges in He and Ne at pressures up to 1500 mbar and in Ar and N_2 up to 1200 mbar. The non-thermal discharges [4] are generated at the gaps between the electrodes, up to 500 mbar the plasma covers the whole electrode system.

In Fig. 3, the breakdown voltages (ignition potentials U_{IP}) of the gases Ne, He, Ar and N_2 of the pressure range 100–1000 mbar are shown.

In order to describe the behavior of the charged particles in the RF field of our system, we use the DC Townsend breakdown theory due to the very small electrode gap width. The motion of the charged particles is drift controlled, because the amplitudes of the electrons as well as the ions exceed $d/2$ (35 μm) [6]. The ion drift amplitudes z_0 (see Fig. 4) were calculated using the following equation:

$$z_0 = \frac{eE_0}{m\omega\sqrt{\omega^2 + v_c^2}}. \quad (1)$$

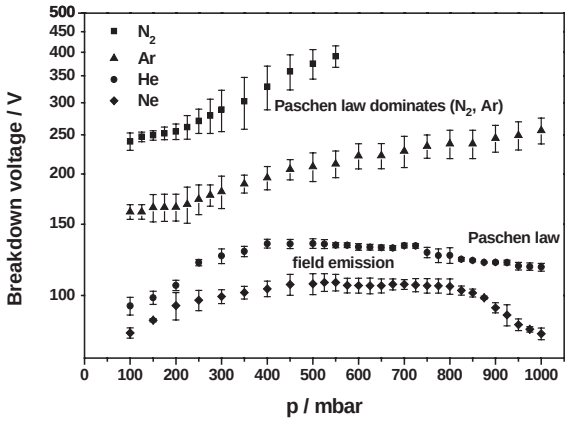

Fig. 3. Experimental breakdown voltages in Ne, He, Ar and N_2 (RF 13.56 MHz, 100–1000 mbar).

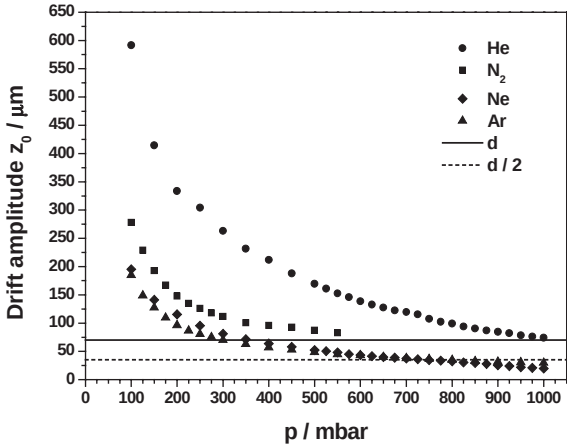

Fig. 4. Ion drift amplitudes calculated with the electric field strengths derived from Fig. 3.

This equation gives the extreme values derived from the solution of the equation of motion (2) including the pressure-dependent Lorentz collisional term in order to regard friction [7]:

$$m\frac{d^2z}{dt^2} + mv_c\frac{dz}{dt} = eE_0 \sin \omega t. \quad (2)$$

The right-hand branches of the Paschen curves of Ar and N_2 and the left-hand branches of Ne and He at pressures higher than 800 mbar obey the Paschen formula [8,9] derived from the Townsend breakdown theory:

$$U_{IP} = \frac{B(pd)}{C + \ln(pd)} \quad (3)$$

with

$$C = \ln\frac{A}{\ln\left((1/\gamma) + 1\right)}. \quad (4)$$

The mentioned branches are fitted with the Paschen formula (curves shown in Fig. 5), the fitted constants are listed in Table 1. The determined B values of the RF field are of the same magnitude, but lower than the B values of the DC field (with the exception of Ne) [8], because the voltages required to initiate and maintain AC discharges decrease strongly in comparison to DC glow discharges with increasing frequency [9]. The strong deviation of the neon B value can partly be explained by the non-matching of the regions of applicability, because some of the ion drift

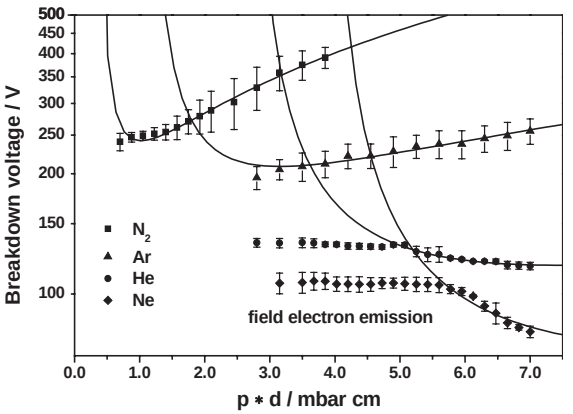

Fig. 5. Fitted Paschen curves in Ne, He, Ar and N_2 (electrode gap width $d = 70$ μm).

Table 1
Fitted constants of the Paschen formula and regions of applicability (B and E/p in $\mathrm{V\,mbar^{-1}\,cm^{-1}}$)

Gas	Experiment (RF)			Literature [8] (DC)	
	B	C	E_{eff}/p	B	E/p
Ne	6.72 ± 0.43	-1.38 ± 0.03	11–20	75	75–300
He	15.73 ± 0.23	-1.02 ± 0.01	17–28	26	15–100
Ar	66.2 ± 1.4	-0.15 ± 0.03	37–70	135	75–450
N_2	237.8 ± 5.2	$+0.98 \pm 0.04$	102–282	256	75–450

amplitudes of Ne do not exceed $d/2$ in the fitted pressure range. Thus, the breakdown controlling regime is a mixture between the high-frequency discharge theory [6,9] and the Townsend breakdown theory.

While the Paschen curves for He and Ne fit very well the experimental data at high pd values, they deviate at lower pd values significantly. Theoretically, higher breakdown voltages are expected due to the growing lack of impact partners with decreasing pd values. Hartherz et al. [10] have shown that with d values in the μm-range the breakdown voltages are increasingly dominated by field electron emission with decreasing pressure, although the used electric field strengths are less than one magnitude below 10^6 V/cm [8].

In Ne, He and Ar at pressures lower than 350 mbar, the discharges show a new pressure-dependent behavior. As can be seen in Fig. 3, in this pressure range the ion drift amplitudes of the three gases exceed not only $d/2$ but also d. Thus, the ignition behavior is again dominated by the Townsend regime, a higher second Townsend coefficient γ represented by a higher secondary ion-electron emission coefficient γ_i in comparison to γ_i at atmospheric pressure contributes to the decrease of the breakdown voltage (see Eq. (4)). Additionally, with decreasing pressure in He and Ar, an increasing contribution of the field electron emission lowers the breakdown voltages. Thus, the voltages measured at low pressures are lower than the expected values given by the Paschen curves fitted at high pressures.

These reasons can explain the additional decrease of the breakdown voltage, but not the special pressure-dependent behavior shown in this pressure range. At the breakdown, the complete surface of the electrodes is covered with a darker diffuse plasma compared to the intense plasma generated only at the gaps between the electrodes at high pressures. Thus, higher breakdown distances are favored to the shortest electrode gap width of 70 μm. The MSE-driven discharges of Ne, He and Ar at pressures lower than 350 mbar represent the left-hand branches of the Paschen curves near the minimum with higher effective d values. The interpretation of this effect is supported by the observation of additional parasite discharges at pressures lower than 350 mbar, which ignite within distances of several millimeters inside the chamber. Therefore, the parasite discharges must represent the right-hand branches of the Paschen curves at high pd values. Since the effective d values are unknown, we are not able to run a new fit with the Paschen formula, which would result in Paschen curves with considerably lower breakdown voltages than the fitted Paschen curves shown in Fig. 5.

Experiments with a new MSE design with an electrode gap width of 25 μm, an electrode thickness of 35 μm and a width of 1350 μm (electrode material: Ni) confirm the observations and interpretations made above. In Ne and He at pressures lower than 350 mbar, the discharges show the same pressure-dependent behavior described above. At pressures between 350 mbar and atmospheric pressure, the discharges are totally dominated by field electron emission. Since we work with $d = 25$ μm in the pd region of 0.25–2.5 mbar cm, we are able to observe in this region the Paschen minima in Ar and N_2. Quantitative results will be published.

4. Applications

With the MSE array as plasma source incorporated into a micro-reactor, the decomposition of the greenhouse gas CF_4 was performed with rates of over 90% at a pressure of 100 mbar in He and N_2. At atmospheric pressure, the abatement rate is still over 70% [5].

Using the sterilization and deposition setup shown in Fig. 2, we successfully deposited SiO_2 layers on various substrates (Si, Cu, polymer films) with a deposition rate of 30 nm/min (9.5 kHz AC bias up to 1000 Vpp). A gas stream of 1% oxygen in helium (100 sccm, working pressure up to 100 mbar) was bubbled through tetraethoxysilane (TEOS) at 0°C.

We also successfully sterilized polymer films (PET, PS and PP) in helium inoculated with 10^6 thermo-resistant spores of the vegetative bacteria *Bacillus cereus* pertaining to the sporulating genus *Bacillus*, *Clostridium* and *Desulfotomaculum* suspended in 0.05 ml. Furthermore, we totally deactivated the same quantity of spores of the fungus *Aspergillus niger* in argon. The spores of these microorganisms are reference spores for the total deactivation by established methods like the treatment with H_2O_2-solution or UV-radiation.

The MSE plasma source provides the reactive species at atmospheric pressure in helium or argon. The AC bias potential (9.5 kHz) accelerates the charged particles, ions and electrons, to the substrate. Thus, the plasma volume is extended by the bias potential towards the substrate. At a pressure of 100 mbar, the entire volume between the MSE array and the substrate is filled with the plasma. Fig. 6 shows that the AC bias rectified to a pulsed DC-(+) bias not only accelerates the electrons resulting in an electron bombardment of the microorganisms on the substrate surface but also lowers the plasma sustaining voltage applied to the MSE array supporting the ignition. The measurement in He (300 sccm, bias 10.4 kHz, +700 V) shows an insufficient sterilization performance. This observation leads to the interpretation that electrons as the only sterilizing agents cannot fulfill the demand of total deactivation.

In the case of an applied DC-(−) bias (10.4 kHz, −700 V) in He (300 sccm), we assumed

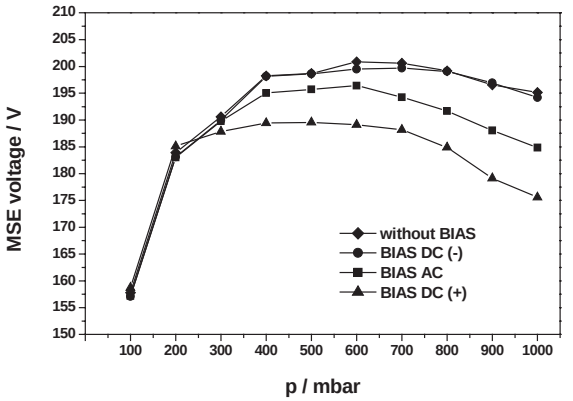

Fig. 6. Measured MSE voltages dependent on pressure and bias (300 sccm Ar, 9.5 kHz, AC-bias 1300 Vpp, DC(+)-, DC(−)-bias ±750 V; $\sigma < 4\%$).

He^+ ions as sterilizing agents and received good sterilization results. The ions also are accelerated towards the substrate, but we can exclude ion bombardment as the dominating sterilization agent, because the kinetic energies of the ions calculated with Eq. (2) are very low. The analogous experiment with helium (300 sccm) and oxygen (3 sccm) showed similar results as the experiment before. Thus, oxygen as a dominating source for reactive species in form of O_2^+ or metastables can be excluded in this special bias option. Further experiments are necessary to quantify the contribution of oxygen to the deactivation.

The best sterilization performance exhibits the gas discharge in a mixture of 300 sccm He with 3 sccm O_2 with a DC-(+) acceleration potential (10.4 kHz, +700 V). In this case, electrons and negatively charged oxygen ions were responsible for the total deactivation of the spores.

UV-radiation as well is not the exclusive sterilization agent because with the bias potential switched off we did not obtain a total deactivation of the spores.

In summary, a mixture of UV-radiation, charged particle bombardment and the presence of radicals and meta-stables originating from the residual gases oxygen or water always present in the vacuum chamber is responsible for the total deactivation of the spores.

5. Conclusions

With the MSE array, we have an alternative atmospheric pressure plasma source with many applications: plasma chemistry (decomposition of waste gases like CF_4), thin film deposition (e.g. SiO_2 layers on various substrates) and sterilization of food packaging materials.

The MSE-driven RF discharges show a special behavior, which differs from conventional high-frequency gas discharges. Due to the very small electrode gap width (25–70 μm), we can describe the behavior of the charged particles in the RF field of our system with the DC Townsend breakdown theory dependent on pressure range and gas type. With decreasing pressure, the gas discharges, especially in Ne and He, are increasingly dominated by field electron emission, which is an advantage of the micro-structured electrode systems, because the breakdown voltage is lowered. With the gained knowledge, we are able to design MSE arrays optimized for a given pressure range and gas.

Acknowledgements

This work was partially supported by the Bundesministerium für Bildung und Forschung (bmb + f), Germany, under Contract No. 03D0070B/6. We also wish to thank our project partners Dr. T. R. Dietrich and A. Freitag of mgt mikroglas technik AG.

References

[1] Scheffler P. Dissertation. Braunschweig, 2001. ISBN 3-89873-239-8.
[2] Geßner C. Dissertation. Braunschweig, 2001. ISBN 3-89873-325-4.
[3] Geßner C, Scheffler P, Gericke K-H. Proceedings of the International Conference on Phenomena in Ionized Gases (XXV ICPIG), vol. 4, Nagoya, 2001. p. 151–2.
[4] Gericke K-H, Geßner C, Scheffler P. Vacuum 2002; 65:291–7.
[5] Baars-Hibbe L, Sichler P, Schrader C, Geßner C, Gericke K-H, Büttgenbach S. Surf Coatings Technol, 2003; 174–175:519–23.
[6] Wiesemann K. Einführung in die Gaselektronik. Stuttgart: Teubner; 1976. p. 267–8.
[7] Reece RJ. Industrial plasma engineering. Bristol: IOP Publishing; 1995. p. 418–9.
[8] Raizer YP. Gas discharge physics. Berlin, Heidelberg: Springer; 1997. p. 56, 133–5.
[9] Grill A. Cold plasma in materials fabrication. New York: IEEE Press; 1994. p. 24–34.
[10] Hartherz P. Dissertation. Darmstadt, 2002. ISBN 3-8322-0413-X.